PHYSICAL REVIEW B **66**, 140507(R) (2002)

Direct measurement of quasiparticle evanescent waves in a dirty superconductor

J. Y. Gu,* J. A. Caballero, R. D. Slater, R. Loloee, and W. P. Pratt, Jr.
Department of Physics and Astronomy, Center for Fundamental Materials Research, and Center for Sensor Materials, Michigan State University, East Lansing, Michigan 48824-1116

(Received 3 July 2002; published 23 October 2002)

We have used a perpendicular-current spin-polarization detector, in the form of a Permalloy-based exchange-biased spin valve, to measure the length scale for penetration of quasiparticles through superconducting-Nb thin films under diffusive transport conditions. In the low-temperature limit, this penetration length is ~16 nm, comparable to the estimated ''dirty-limit'' zero-temperature coherence length of our Nb films.

DOI: 10.1103/PhysRevB.66.140507 PACS number(s): 74.25.Fy, 74.50.+r, 72.25.Ba

Electron transport across the interface between a superconductor (S) and a ferromagnetic (F) metal is an area of active interest. For example, the consequences of Andreev reflection[1] upon the injection of a spin-polarized current from F into S have been used to measure the degree of spin polarization of various ferromagnets,[2–4] including the highly spin-polarized half-metallic ferromagnet CrO_2.[3,5–7] Andreev reflection occurs when an electron enters S and is reflected as a hole, adding a Cooper pair to the S condensate. Although Andreev reflection is typically thought of as an ''interfacial'' process, it actually takes place over a finite length scale l_{qp} in S as quasiparticles with energy E less than Δ (pair potential) enter S as ''evanescent'' waves.[8] As pointed out recently,[9] spin-polarized transport in S occurs only via single quasiparticle processes, and thus l_{qp} should be derivable from spin-polarized transport measurements. In this communication, we report direct measurments of l_{qp} for quasiparticle penetration through S in the low-temperature limit under diffusive conditions.

Two other length scales can affect the properties of S/F interfaces, the spin-diffusion lengths l_{sf} (''spin-flip length'') in the F and S metals. Theoretical work[10–12] on S/F interfaces focuses on l_{sf}^F, which contributes to the effective S/F interface resistance via a ''spin-accumulation'' process in F. This length appears only indirectly in our present study, where we have chosen F-layer thicknesses much larger than l_{sf}^F. The spin-diffusion lengths in the normal (N) and superconducting states of a S metal were recently predicted to be the same, $l_{sf}^N = l_{sf}^S$.[13] Because of Andreev reflection, we will see that l_{qp} in our proximity-coupled superconductor is less than its l_{sf}^N.

The only prior attempt to measure l_{qp} in a conventional superconductor using spin-polarized transport[14] employed a $F1$/Nb/$F2$ spin-transistor geometry that suffered from important problems. The current distribution of interest was highly nonuniform, the voltage response was not linear with applied current, and the relative magnetic order of the two F layers was not under good control in the antiparallel state. Also the measurements were restricted to the narrow temperature (T) range $0.985 \lesssim T/T_c \lesssim 1.0$, where T_c is the superconducting transition temperature of the Nb. For this range of T/T_c, less than 20% of the electrons impinging on S satisfy the $E<\Delta$ criterion for evanescent-wave behavior. Thus it is not surprising that extrapolation to the $T=0$ limit gave $l_{qp} \sim 2$ nm, a very low value relative to expectations. In the present paper we measure l_{qp} in superconducting Nb using a technique that provides a uniform current distribution, ohmic response, good control of the antiparallel (AP) and parallel (P) magnetic order of the two F layers, and a lowest temperature range of $T/T_c \lesssim 0.3$ for which over 99.7% of electrons impinging on S satisfy the $E<\Delta$ criterion. The resulting $T=0$ value of l_{qp} is an order of magnitude larger than that estimated from the spin transistor.[14] Our technique provides a way to systematically study how l_{qp} varies with temperature and S thickness for a variety of superconductors.

We used an adaptation of our perpendicular-current (CPP) exchange-biased spin valve,[15] as shown in Fig. 1, where lithographic patterning of the pillar ensures that the current density through the middle Nb layer remains unchanged when it turns superconducting. The $Fe_{50}Mn_{50}$ layer ''pins'' the adjacent Permalloy (= ''Py'') layer via exchange bias so that its magnetization M remains fixed in weak magnetic fields that can reorient M of the ''free'' Py layer, allowing good control of the relative P and AP states of these two F layers. For CPP measurements, the important parameters are specific resistances AR_{AP} and AR_P, where A is the 75 μm $\times$ 75 μm area of CPP current flow, and R_{AP} and R_P are the CPP resistances in the AP and P states of the two F layers, respectively. The specific magnetoresistance $A\Delta R$ $[=A(R_{AP}-R_P)]$ will decrease if spin memory is lost as the

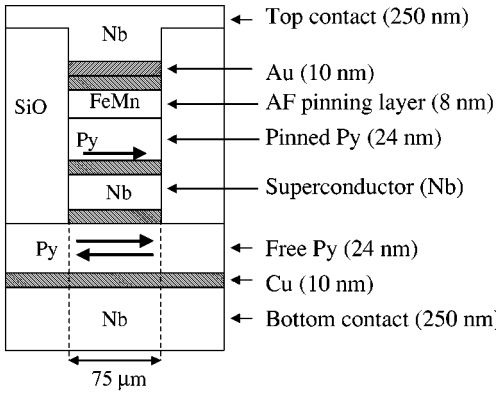

FIG. 1. Diagram of CPP exchange-biased spin valve structure in the form of a 75 μm$\times$75 μm pillar. There are four 10-nm-thick Cu layers, and Py=$Ni_{84}Fe_{16}$.

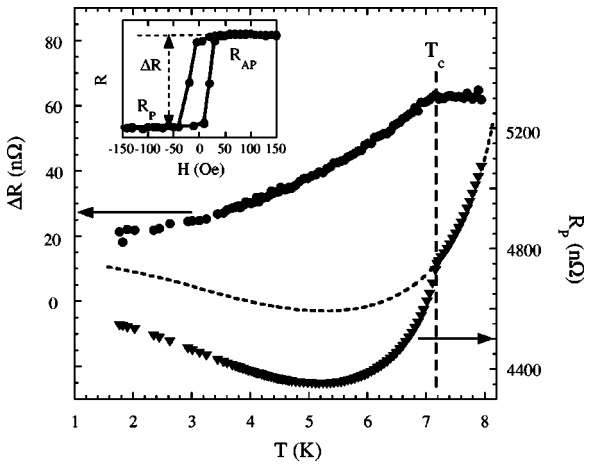

FIG. 2. Temperature dependences of ΔR (●, left-hand ordinate) and R_P (▼, right-hand ordinate) for $t_{Nb}=60$ nm. For comparison, R_P of a $t_{Nb}=15$ nm sample is shown as a dashed curve. Inset shows the CPP-resistance vs magnetic field at 4.2 K for the $t_{Nb}=60$ nm sample as the magnetization of the ''free'' Py layer cycles between its antiparallel (AP) and parallel (P) orientations with respect to that of the ''pinned'' Py layer. These values of R_P and ΔR at 4.2 K can be read from the main figure.

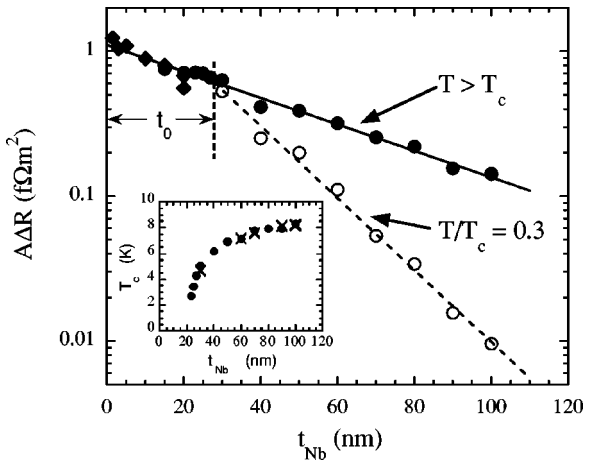

FIG. 3. $A\Delta R$ vs t_{Nb} in the normal ($T>T_c$) and superconducting ($\bigcirc, T/T_c=0.3$) states. For $T>T_c$, ♦ and ● represent, respectively, 1 mm×1 mm samples with $t_{Nb}\leqslant 20$ nm (Ref. 15) and 75 μm×75 μm pillars with $t_{Nb}\geqslant 15$ nm. The solid and dashed lines are least-squares fits to the data for $T>T_c$ and $T/T_c=0.3$, respectively. t_0 is explained in the text. Inset: ● depicts the dependence of T_c on t_{Nb}; × is for the case where the two Cu layers on either side of the middle Nb layer are missing.

current traverses the middle Nb layer. The CPP resistance exhibits no observable dependence upon applied current even when this Nb layer is superconducting, except at higher current densities ($\sim$100 A/cm^2) for T very near T_c of the outer Nb contacts. The middle Nb layer was separated from the two Py layers by two Cu layers of $t_{Cu}=10$ nm thickness to eliminate an observed $\sim$50% drop in ΔR when Nb and Py are in direct contact and to allow a direct comparison with our earlier work on spin-memory loss in nonsuperconducting thin Nb layers.[15]

The inset to Fig. 2 shows the magnetic-field dependence of the CPP resistance at 4.2 K for a superconducting $t_{Nb}=60$ nm sample. This minor hysteresis loop demonstrates the well-established AP and P states of the two Py layers in modest magnetic fields. In most of the experiments $\sim\pm 100$ Oe fields were adequate for this purpose. The main part of Fig. 2 shows the T dependence of ΔR and R_P. For $T>T_c$, ΔR is temperature independent. At T_c, ΔR begins to decrease with decreasing T in the superconducting state. At $T\approx 1.5$ K, ΔR is about 1/3 of its value at T_c, implying significant residual spin-polarized quasiparticle penetration through this Nb layer. Note that our detector responds to a reduced quasiparticle penetration through S as a loss of spin memory (a lower ΔR).

The behavior of R_P is more complex. At T_c, R_P exhibits a discontinuity in slope, with R_P initially decreasing rapidly for $T<T_c$. Note that ΔR and R_P imply the same value of T_c, and this agreement applies to all values of t_{Nb}.[16] The dashed curve shows the T dependence of R_P for a $t_{Nb}=15$ nm sample where the Nb layer is not superconducting for $T\gtrsim 1.5$ K. Separate experiments indicate that this resistance-minimum behavior originates mostly at the interfaces between the multilayer and the outer 250-nm-thick Nb layers that have $T_c\geqslant 9.1$ K. Above T_c of the 60-nm sample, the two R_P data sets look similar.[17] Below T_c, the difference between them shows the effect on R_P of this middle Nb layer becoming superconducting. Further analysis of the R_P behaviors will be published elsewhere.[18]

In Fig. 3, $A\Delta R$ decays as a simple exponential with t_{Nb} for both the normal and superconducting ($T/T_c=0.3$) states. The inset shows that T_c depends upon t_{Nb} due to the proximity of the two Py layers. Based upon our earlier studies with such a spin-polarization detector,[15] we define an ''effective spin-polarized quasiparticle penetration length'' l_{qp}^{eff} in the Nb for the two states using $A\Delta R\propto\exp(-t_{Nb}/l_{qp}^{eff})$. For the normal state, the two sets of data, for earlier 1 mm×1 mm samples (♦) (Ref. 15) and present 75 μm×75 μm pillars (●), are in very good agreement in their region of overlap; and they combine to give $l_{qp}^{eff}=48\pm 3$ nm ($\equiv l_{sf}^{Nb}$), which agrees well with $l_{sf}^{Nb}=25^{+\infty}_{-5}$ nm obtained earlier for only the 1 mm×1 mm samples. We assume that l_{sf}^{Nb} in the normal state is due to spin-orbit scattering, because in our studies of normal metals,[15] l_{sf} decreased systematically with increasing Z (V→Nb→W) as would be expected for spin-orbit scattering. However, this value of l_{sf}^{Nb} is much smaller than the $\sim$800 nm obtained in the spin-transistor experiments for Nb samples of similar residual resistivity.[14] Thus perhaps magnetic impurity scattering contributions to l_{sf}^{Nb} cannot be ruled out for our Nb films.[19] For the superconducting state with $T/T_c=0.3$, we obtain $l_{qp}^{eff}=17.5\pm 0.6$ nm, which provides an approximate measure of the length scale for quasiparticle penetration into the Nb prior to Andreev reflection at this relatively low temperature. However, since l_{qp}^{eff} is a combination of the actual length scale for quasiparticle penetration (l_{qp}) and l_{sf}^{Nb}, further analysis is needed to extract l_{qp}.

For our Nb the residual resistivity $\rho_{Nb}\approx 60\pm 10$ nΩ m at 12 K. From $\rho_{Nb}\lambda_{Nb}=0.38$ fΩ m^2,[20] where λ_{Nb} is the elastic mean free path, we obtain $\lambda_{Nb}\approx 6$ nm. Hence our samples have $\lambda_{Nb}\ll t_{Nb}$, implying that the motion of the quasiparti-

cles is diffusive. In this diffusive and low-T limit, one has in the superconducting state that $l_{qp}^{eff}=\sqrt{D\tau_{eff}}$, where D is the electron diffusion constant and τ_{eff} is an effective time containing contributions from both ''spin-orbit'' scattering and Cooper-pair formation via Andreev reflection for quasiparticles with $E \ll \Delta$. If the two processes are independent, then their rates add, giving the simple result $(l_{qp}^{eff})^{-2}=(l_{qp})^{-2}+(l_{sf}^{Nb})^{-2}$. We obtain $l_{qp}=18.8\pm 0.8$ nm for $T/T_c=0.3$, which is an upper bound on its $T=0$ value l_{qp}^0. One can estimate the Ginzberg-Landau $T=0$ dirty-limit coherence length for our Nb using $\xi(0)\approx 0.86\sqrt{\lambda_{Nb}\xi_0}$, where ξ_0 is the clean-limit coherence length for Nb ($\sim$40 nm).[8] We obtain $\xi(0)\approx 13$ nm, comparable to our value of l_{qp}. This is the central result of this paper: the penetration length for diffusing spin-polarized quasiparticles with $E \ll \Delta$ appears to be close to the $T=0$ dirty-limit coherence length and is not as short as estimated earlier.[14] Our work demonstrates that under diffusive conditions with $E \ll \Delta$ the length scale of the polarized evanescent-wave penetration is $\sim\xi(0)$, a result that had been anticipated for diffusing unpolarized quasiparticles.[21]

In Fig. 3 the $T/T_c=0.3$ line joins the $T>T_c$ line at $t_{Nb}\approx 28$ nm. At this thickness Δ no longer acts as a ''barrier'' to quasiparticle penetration. To take this Δ depression into account, we adopt the following simple model to compute the T dependence of ΔR: let Δ be a rectangular barrier of reduced width $(t_{Nb}-t_0)$ and constant height $\Delta_b(T)$, where $\Delta=0$ everywhere outside the barrier. Thus at the line-joining point in Fig. 3, the effective barrier width is zero, giving $t_0\approx 28$ nm, a reasonable value in comparison to $\sim 2\xi(0)$. This severe depression of Δ inside S over a distance of $\sim\xi(0)$ from the two S/F interfaces is similar to that observed in the Au/$NbSe_2$ system.[22,23] We also assume that the barrier height $\Delta_b(T)$ has the BCS temperature dependence and is proportional to $T_c(t_{Nb})$,[25] the actual T_c of the Nb layer of thickness t_{Nb}.

The next step in modeling the T behavior of ΔR is to divide the flux of quasiparticles entering S from F into two parts: the fractions (Φ) with $E>\Delta_b$ and $E<\Delta_b$. In the low-voltage-biased limit that is applicable to our experiments, we have for the former[24]

$$\Phi_{E>\Delta_b}=2\int_{\Delta_b(T)}^{+\infty}\left(-\frac{\partial f}{\partial E}\right)dE=2f[\Delta_b(T)], \qquad (1)$$

where f is the Fermi-Dirac distribution function and $\Phi_{E<\Delta_b}=1-\Phi_{E>\Delta_b}$. Note that in the $T=0$ limit, one has $\Phi_{E>\Delta_b}=0$.

To compare ΔR data for different values of t_{Nb}, we normalize each ΔR data set at fixed t_{Nb} $(=\Delta R_{norm})$ to its value at T slightly above T_c, where ΔR is mostly independent of T. The resulting quantity ΔR_{norm} satisfies $0\leqslant\Delta R_{norm}\leqslant 1$ for $0\leqslant T/T_c\leqslant 1$. Since we want to emphasize those quasiparticles with $E<\Delta_b$, we subtract from ΔR_{norm} the contribution of quasiparticles with $E>\Delta_b$. If the quasiparticle transmission probability across the barrier is unchanged in the superconducting state for $E>\Delta_b$, then this subtractive correction is simply $\Phi_{E>\Delta_b}=2f[\Delta_b(T)]$. Here we have ignored for $E>\Delta_b$ the possibility of Andreev reflection and relaxation of quasiparticles into Cooper pairs by other processes. Thus in Fig. 4 we plot $\Delta R_{E<\Delta_b}=\{\Delta R_{norm}-2f[\Delta_b(T)]\}$ vs T/T_c, for 30 nm$\leqslant t_{Nb}\leqslant$100 nm.

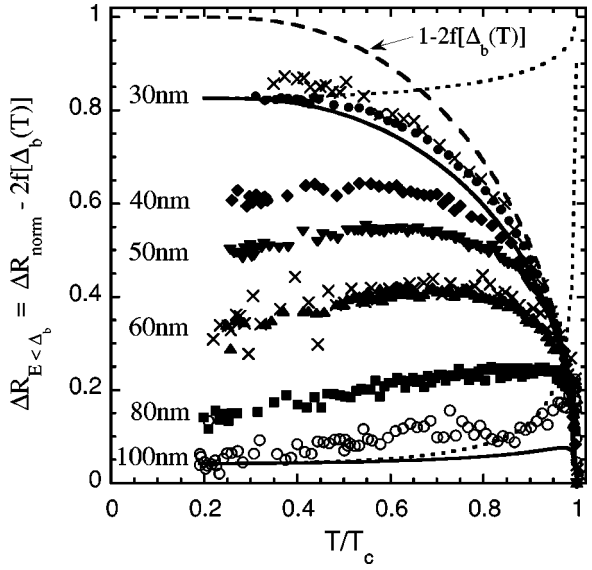

FIG. 4. $\Delta R_{E<\Delta_b}=\Delta R_{norm}-2f[\Delta_b(T)]$ vs T/T_c for different thickness Nb samples where ΔR_{norm} is a normalized form of the ΔR data, f is the Fermi-Dirac distribution function and T_c is the actual transition temperature for each value of t_{Nb}. The $\times$ symbols are for the case where the two Cu layers on either side of the middle Nb layer are missing for $t_{Nb}=30$ and 60 nm. The solid, dashed, and dotted curves are explained in the text.

In Fig. 4, the behaviors of $\Delta R_{E<\Delta_b}$ for the extremes of t_{Nb} are simple. For small t_{Nb}, the quasiparticles with $E<\Delta_b$ have a very small probability of forming Cooper pairs and thus $\Delta R_{E<\Delta_b}\approx 1-2f[\Delta_b(T)]$, represented by the dashed curve. Indeed, the $t_{Nb}=30$ nm data are reasonably close to this dashed curve. For the other extreme of very large t_{Nb}, the quasiparticles with $E<\Delta_b$ have a very high probability of forming Cooper pairs, causing $\Delta R_{E<\Delta_b}\approx 0$. As expected, the $t_{Nb}=100$ nm data are reasonably close to this limit. In Fig. 4 and in the inset to Fig. 3, the $\times$ symbols represent the case where the two Cu layers on either side of the middle Nb layer are missing. In both figures these data agree reasonably well with those for $t_{Cu}=10$ nm, implying that the presence of the Cu layers does not affect our conclusions about the quasiparticle transport in Nb.

To understand better the T dependence of $\Delta R_{E<\Delta_b}$, we assume in the diffusive limit that the quasiparticle penetration length obeys $l_{qp}(T)=\sqrt{D\tau_A(T)}$ where $\tau_A(T)$ is the characteristic time for Andreev reflection with $\tau_A(T)\propto 1/\Delta_b(T)$ from an ''uncertainty-principle'' argument. Here we ignore any dependence of $l_{qp}(T)$ on E, essentially taking the $E=0$ limit for $l_{qp}(T)$. We obtain

$$\Delta R_{E<\Delta_b}=\{1-2f[\Delta_b(T)]\}\times\{e^{-(t_{Nb}-t_0)[\sqrt{[l_{sf}^{Nb}]^{-2}+[l_{qp}(T)]^{-2}}-[1/l_{sf}^{Nb}]]}\}. \qquad (2)$$

The two dotted curves in Fig. 4 represent the second term in the right-hand side of Eq. (2) for $t_{Nb}=30$ and 100 nm, associated with the T dependence of l_{qp}. The two solid curves are the corresponding complete fits to the data by Eq. (2) for $T/T_c \lesssim 0.3$. At intermediate temperatures, the fit to the 30-nm data is reasonable, but the fit to the 100-nm data is worse, although the overall T behavior is similar to the data. These fits show that the $\Delta R_{E<\Delta_b}$ data represent a competition with decreasing T between the increasing flux of quasiparticles with $E<\Delta_b$ and the decreasing transmission probability associated with the reduction of $l_{qp}(T)$. More extensive fits of Eq. (2) to all the data for $T/T_c \lesssim 0.3$ were done, but at intermediate temperatures the fits fell below the data of Fig. 4, becoming progressively worse as t_{Nb} increased. For each value of t_{Nb}, l_{qp}^0 $[=l_{qp}(0)]$ and t_0 were adjusted within the range 16.5 ± 1 nm and 26.5 ± 3 nm, respectively, to obtain the fits. This value of l_{qp}^0 is remarkably close to $\xi(0)$ (13 nm) estimated above. Clearly further theoretical work is needed that includes better modeling of the spin-memory-loss detector in its AP and P states under diffusive quasiparticle transport through a realistic Δ barrier at all energies.

In conclusion, we have used the magnetoresistance of a perpendicular-current exchange-biased spin valve to measure the penetration length of spin-polarized quasiparticles as they diffusively traverse superconducting Nb. In the $T=0$ limit, the length scale for this penetration is $\sim$16 nm, comparable to the estimated zero-temperature dirty-limit coherence length. Theoretical work is needed to model the spin-polarization detector and the temperature dependence of the spin-polarized transport.

We gratefully acknowledge useful discussions with N. O. Birge, C. J. Lambert, B. E. Nadgorny, M. I. Dykman, S. H. Tessmer, and J. Bass. This work was supported in part by the MSU CFMR, MSU CSM, and NSF under Grants Nos. DMR-98-20135 and DMR-98-09688.

*Present address: Materials Science Division, Argonne National Lab., Argonne, IL 60439-4845.

[1] A.F. Andreev, Zh. Eksp. Teor. Fiz. **46**, 1823 (1964) [Sov. Phys. JETP **19**, 1228 (1964)].

[2] M.J.M. de Jong and C.W.J. Beenakker, Phys. Rev. Lett. **74**, 1657 (1995).

[3] R.J. Soulen *et al.*, Science **282**, 85 (1998).

[4] S.K. Upadhyay *et al.*, Phys. Rev. Lett. **81**, 3247 (1998).

[5] Y. Ji *et al.*, Phys. Rev. Lett. **86**, 5585 (2001).

[6] W.J. DeSisto *et al.*, Appl. Phys. Lett. **76**, 3789 (2000).

[7] Y. Ji *et al.*, Phys. Rev. B **64**, 224425 (2001).

[8] M. Tinkham, *Introduction to Superconductivity* (McGraw-Hill, New York, 1996), and references therein.

[9] R.L. Merrill and Q. Si, Phys. Rev. Lett. **83**, 5326 (1999).

[10] V.I. Fal'ko, A.F. Volkov, and C. Lambert, Phys. Rev. B **60**, 15 394 (1999).

[11] F.J. Jedema *et al.*, Phys. Rev. B **60**, 16 549 (1999).

[12] W. Belzig *et al.*, Phys. Rev. B **62**, 9726 (2000).

[13] T. Yamashita *et al.*, Phys. Rev. B **65**, 172509 (2002).

[14] M. Johnson, Appl. Phys. Lett. **65**, 1460 (1994).

[15] W.J. Park *et al.*, Phys. Rev. B **62**, 1178 (2000).

[16] For these t_{Nb}, this CPP determination of T_c agrees with T_c values obtained by current-in-plane resistance measurements (transition to $R=0$) on separate exchange-biased spin valves where the outer Nb-contact layers were thin enough ($\sim$5 nm) not to be superconducting.

[17] For comparison purposes, an additive constant was applied to the $t_{Nb}=15$ nm data to bring it into coincidence with the $t_{Nb}=60$ nm data for $T>T_c$.

[18] J.Y. Gu *et al.* (unpublished).

[19] H.L. Zhao and W. Hershfield, Phys. Rev. B **52**, 3632 (1995).

[20] H.W. Weber *et al.*, Phys. Rev. B **44**, 7585 (1991).

[21] T.Y. Hsiang and J. Clarke, Phys. Rev. B **21**, 945 (1980), and reference therein.

[22] S.H. Tessmer *et al.*, Phys. Rev. Lett. **77**, 924 (1996), and references therein.

[23] A.D. Truscott, R.C. Dynes, and L.F. Schneemeyer, Phys. Rev. Lett. **83**, 1014 (2000).

[24] G.E. Blonder, M. Tinkham, and T.M. Klapwijk, Phys. Rev. B **25**, 4515 (1982), and references therein.

[25] We used the approximation for $\Delta(T)/T_c$ shown in Ref. 12 (see Ref. 23 therein), where $\Delta(0)/T_c=1.76$. To take account of the "strong-coupling" for Nb, $\Delta(0)/T_c$ was increased by 10%. See A.V. Pronin *et al.*, Phys. Rev. B **57**, 14 416 (1998), and references therein.